Three-Dimensional Quantitative Assessment of Ablation Margins Based on Registration of Pre- and Post-Procedural MRI and Distance Map

HHS Public Access

Author manuscript

Int J Comput Assist Radiol Surg. Author manuscript; available in PMC 2016 June 06.

Published in final edited form as:

Int J Comput Assist Radiol Surg. 2016 June ; 11(6): 1133–1142. doi:10.1007/s11548-016-1398-z.

Three-dimensional quantitative assessment of ablation margins based on registration of pre- and post-procedural MRI and distance map

Soichiro Tani,
Department of Radiology, Brigham and Women's Hospital and Harvard Medical School 75 Francis Street, Boston, MA 02115, USA, Tel.: +1-617-732-7389, Fax: +1-617-582-6033.
Biomedical Innovation Center and Department of Surgery, Shiga University of Medical Science Seta Tsukinowa-Cho, Otsu, Shiga, 520-2192, Japan

Servet Tatli,
Department of Radiology, Brigham and Women's Hospital and Harvard Medical School 75 Francis Street, Boston, MA 02115, USA, Tel.: +1-617-732-7389, Fax: +1-617-582-6033

Nobuhiko Hata,
Department of Radiology, Brigham and Women's Hospital and Harvard Medical School 75 Francis Street, Boston, MA 02115, USA, Tel.: +1-617-732-7389, Fax: +1-617-582-6033

Xavier Garcia-Rojas,
Texas Medical Center, 2450 Holcombe Blvd. Suite X, Houston, TX 77021, USA

Olutayo I. Olubiyi,
Department of Radiology, Brigham and Women's Hospital and Harvard Medical School 75 Francis Street, Boston, MA 02115, USA, Tel.: +1-617-732-7389, Fax: +1-617-582-6033

Stuart G. Silverman, and
Department of Radiology, Brigham and Women's Hospital and Harvard Medical School 75 Francis Street, Boston, MA 02115, USA, Tel.: +1-617-732-7389, Fax: +1-617-582-6033

Junichi Tokuda
Department of Radiology, Brigham and Women's Hospital and Harvard Medical School 75 Francis Street, Boston, MA 02115, USA, Tel.: +1-617-732-7389, Fax: +1-617-582-6033

Soichiro Tani: stani@partners.org; Servet Tatli: statli@partners.org; Nobuhiko Hata: nhata@partners.org; Olutayo I. Olubiyi: oolubiyi@partners.org; Stuart G. Silverman: sgsilverman@partners.org; Junichi Tokuda: jtokuda@partners.org

Abstract

Purpose—Contrast-enhanced MR images are widely used to confirm the adequacy of ablation margin after liver ablation for early prediction of local recurrence. However, quantitative assessment of the ablation margin by comparing pre- and post-procedural images remains

Compliance with Ethical Standards The study protocol has been reviewed and approved by the institutional review board at Brigham and Women's Hospital (IRB# 2002P001166), and was HIPAA compliant. Informed consent was waived by our institutional review board. NH has a financial interest in Harmonus, a company developing Image Guided Therapy products. NH's interests were reviewed and are managed by Brigham and Women's Hospital and Partners HealthCare in accordance with their conflict of interest policies.

challenging. We developed and tested a novel method for three-dimensional quantitative assessment of ablation margin based on non-rigid image registration and 3D distance map.

Methods—Our method was tested with pre- and post-procedural MR images acquired in 21 patients who underwent image-guided percutaneous liver ablation. The two images were co-registered using non-rigid intensity-based registration. After the tumor and ablation volumes were segmented, target volume coverage, percent of tumor coverage, and Dice Similarity Coefficient were calculated as metrics representing overall adequacy of ablation. In addition, 3D distance map around the tumor was computed and superimposed on the ablation volume to identify the area with insufficient margins. For patients with local recurrences, the follow-up images were registered to the post-procedural image. Three-D minimum distance between the recurrence and the areas with insufficient margins were quantified.

Results—The percent tumor coverage for all non-recurrent cases was 100%. Five cases had tumor recurrences, and the 3D distance map revealed insufficient tumor coverage or a 0-millimeter margin. It also showed that two recurrences were remote to the insufficient margin.

Conclusions—Non-rigid registration and 3D distance map allows us to quantitatively evaluate the adequacy of the ablation margin after percutaneous liver ablation. The method may be useful to predict local recurrences immediately following ablation procedure.

Keywords

Liver ablation; MRI; Image-guided intervention; ablation margin; image registration

1 Introduction

Image-guided percutaneous thermal ablations, such as radiofrequency ablation (RFA) [8,5,48,40], cryoablation [8,5,46,39], and microwave coagulation therapy (MCT) [8,5,27,43,22], are promising alternatives to surgical resection for liver tumor treatment. There has been a strong demand for those thermal ablations; while the liver is the dominant metastatic site for gastrointestinal primary tumors [14], and the origin of the sixth most common cancer worldwide [47], curative treatment options for liver tumors are currently limited to surgical resection and thermal ablations. Thermal ablations are particularly important for those who are not eligible for surgical resection. Thermal ablations allow ablating tumor under image guidance without major incisions, and thus provide low morbidity rates with less complications and hospitalization [8,9]. Although thermal ablation methods are effective, particularly for tumors less than 3 cm in diameter [13], recurrences occur. Achievement of an adequate ablation margin is an important common denominator of complete ablation and therefore the success of the therapy [32,18,44]. Adequacy of the ablation margin is assessed by post-procedural contrast-enhanced computed tomography (CT) or magnetic resonance imaging (MRI) [4,19,20,29]. However, the tumor is often obscured on the post-procedural images making it difficult to evaluate the ablation margin using a post-procedural image alone. For this reason, radiologists typically estimate the ablation margin by comparing the pre- and post-procedural images side by side using anatomical landmarks and mental registration. This practice is cumbersome and may underestimate or overestimate the ablation margins within a three-dimensional (3D) volume.

Alternatively, pre- and post-procedural images can be registered to one another using image registration techniques [17,50,2,12,35]. Image registration techniques can correct the misalignment between the two images, allowing radiologists to compare the ablation volume and the tumor directly; hence, this may improve the prediction of inadequate ablation coverage and may allow for more prompt retreatment in the hope of achieving improved local tumor control. Particularly, non-rigid registration techniques can compensate deformation of the anatomy between the two exams, and offer better registration accuracy than conventional rigid registration techniques [10,36]. Kim *et al* successfully used a non-rigid registration technique for the evaluation of ablation margins in their clinical study [17]; the deformable registration allowed them not only to examine overall ablation margin, but also to localize the thinnest margin with respect to the tumor, and correlate it with local recurrences. However, their approach to the localization of the thinnest margin relies on radiologists' visual assessment of the margin and encoding using a spherical coordinated system fitted to the ablation volume. While this was a novel way to assess the ablation margins, it can still be objective especially when the ablation volume is not a complete sphere.

In this study, we developed a new method to quantitatively assess the ablation margin and correlate it with local recurrence. The feasibility of the method was evaluated using pre- and post-procedural images, and follow-up images of patients who underwent image-guided percutaneous ablations. Our method generates a 3D distance map around the tumor, and overlays it on the ablation volume to visualize the distribution of the ablation margin on the surface of the ablation volume after registering the pre- and post-procedural images. Furthermore, the method can calculate the distance between the area with a positive or the thinnest margin and the local recurrence to correlate them.

2 Methods

2.1 Patient Selection

The study protocol has been reviewed and approved by the institutional review board, and was HIPAA compliant. A total of 208 hepatic percutaneous ablation procedures were performed between January 1, 2008 and December 31, 2012. Patients were not limited to certain image guidance modalities, thermal ablation modalities, or tumor histologies; the ablations were performed under CT, MR, or positron emission tomography (PET)/CT guidance using MCT, RFA, or cryoablation techniques.

We used inclusion criteria shown in Fig. 1 to avoid any confounding factor that might cause local recurrences and ensure that the patient underwent necessary follow-up exams.

After all exclusions, a total of 21 hepatic tumors (mean tumor volume 8.0 cm^3, range 0.4–40.2 cm^3; mean greatest tumor diameter 2.0 cm, range 0.9–4.1 cm^3) in 19 patients (mean age 60, range 42–84; 8 female, 14 male) were enrolled. The characteristics of target lesions including primary origin and their sizes, and ablation modalities used to treat them are shown in Table 1.

2.2 Pre- and Post-Procedural Imaging and Follow-up

All pre-procedure MRI exams were performed within 30 days (mean 11.5 days, range 1–27 days) before the procedure using one of the following 1.5T or 3T MRI scanners with a phased-array body coil: MAGNETOM Aera, MAGNE-TOM Trio, or MAGNETOM Verio (Siemens AG, Munich, Germany); or Signa EXCITE 1.5T, Signa HDx 1.5T, Signa HDx 3T, Signa HDxt 1.5T, or Signa HDxt 3T (GE Healthcare, Waukshesha, WI). CE-MR images were acquired using a T1-weighted 3D gradient-echo sequence before and 30, 60, and 90 seconds after intravenous administration of 0.1 mmol/kg of gadopentetate dimeglumine (Magnevist, Bayer HealthCare Pharmaceuticals, Berlin, Germany). The post-procedure MR images were also acquired in the same manner, within 72 hours following the procedure. The patients were followed up with CE-MR or CT images at regular intervals, at least for a year. We defined local recurrence as a post-procedural development of tumor adjacent to or within ablation area [33,32]. Among the 21 patients, recurrences were found in five patients.

2.3 Ablation

Patients underwent one of the following procedures: cryoablations (n=12) performed using argon-gas-based cryotherapy applicators (IceRods and Ice-Spheres, Galil Medical Ltd., Yokneam, Israel) with two 15-minute freezing cycles separated by a 10 minute passive thaw; radiofrequency ablations (n=7) performed using an RF generator (Cool-tip system, Covidien, Mansfield, MA) at 120 watts with impedance control for 12 minutes; microwave ablation (n=2) performed using a needle-like applicator (AMICA, HS Medical, Boca Raton, FL) with 80 watts for 15 minutes.

2.4 Non-Rigid Registration and Segmentation of Tumor and Ablation Zone

The pre-procedural CE-MR and follow-up images were registered to the post-procedural images. We used a non-rigid B-Spline registration technique, which has been tested extensively in our group and provided reasonable registration accuracy in several clinical applications [10,37,11]. The B-Spline registration can correct for deformation of the liver, and thus it can provide better alignment than the affine registration technique alone (4.1 mm vs 11.04 mm; $p < 0.05$)[10]. The pre- and post-procedural CE-MR images of the 21 cases were loaded onto open-source image-processing and visualization software (3D Slicer version 4; http://www.slicer.org/) on a Linux workstation. Before applying non-rigid registration, the intensity bias of the MR images within the liver was corrected using the N4ITK Bias Correction module in 3D Slicer with a grid of 5×5×5. A region of interest (ROI) was defined manually on the liver for the bias correction. Registration was performed using the General Registration module in 3D Slicer 4. The following steps were used: alignment of the center of the region of interest (ROI), rigid registration, affine registration, and non-rigid B-Spline registration. We used the aforementioned ROI of the liver for registration. The B-Spline grid was set to be 6 per direction. We used a hierarchical registration approach[11], where the degree-of-freedom (DOF) of registration transform was gradually increased through the hierarchical process. We included rigid (6-DOF), affine (12-DOF), and B-spline (125-DOF) in this process. The registration accuracy was evaluated using target registration error (TRE). The TRE was calculated based on five corresponding

anatomical landmarks manually selected on the pre-procedural, post-procedural, and follow-up images.

Once the images were registered, the tumor, and ablation zone were segmented manually on the pre- and post-procedural images by an abdominal surgeon (S. Tani), and were reviewed and revised by a board-certified radiologist (S. Tatli). Tumors were identified as areas of abnormal enhancement or washout on the pre-procedural CE-MRI. Ablation zone was identified by new unenhancing area encompassing the tumor on the post-procedural CE-MR images.

2.5 Assessment of Ablation Margin

The adequacy of ablation margin was evaluated using a volumetric approach used in our previous study [45], and a distance -based approach newly introduced in this study.

Volumetric Approach—The following three metrics were calculated: 1) Percent of target volume coverage defined as the percentage of ablation zone within the target volume, which combines the volume of the tumor and the desired margin; 2) Percent of tumor volume coverage defined as the percentage of ablation zone within the tumor; and 3) Dice Similarity Coefficient (DSC) that measures the agreement between the target volume and the ablation zone. The percent of target volume coverage, percent of tumor volume coverage, and DSC can be formulated as (% target volume coverage) = $(a/b) \times 100$, (% tumor volume coverage) = $(a/c) \times 100$, and (DSC) = $(2a/(2a + b + d)$ respectively, where a is the volume common to the tumor and the ablation zone, b is the volume of the target, c is the volume of the tumor, and d is the volume of the ablation zone. The target volume was defined as the tumor and a 10-mm volumetric margin extending in all directions perpendicular to the manually segmented tumor surface [45], which was calculated using the ErodeDilateLabel module in 3D Slicer software.

Distance-Based Approach—The area with insufficient ablation margin (positive margin or thinnest margin) was identified using a 3D distance map superimposed on the 3D surface model of the ablation volume. The distance map is a volumetric image computed for a given region (i.e. tumor); each voxel represents the minimum Euclidian distance from the voxel to the region (Fig. 2). By computing a distance map of the tumor region and superimposing it on the surface of the ablation zone, one can estimate the minimum distance from each point on the ablation volume surface to the tumor surface. Therefore, the superimposed distance map represents the distribution of the thickness of ablation margin (Fig. 2). We defined the area with a distance equal to zero or positive margin as an area of insufficient margin. The minimum distance value was recorded as a thinnest margin. We used an algorithm to compute the Euclidian distance map proposed by Maurer *et al* [28] available in the Insight Segmentation and Registration Toolkit (http://itk.org/).

2.6 Assessment of Local Recurrence

To assess the local recurrence, the follow-up image was registered to the post-procedural image using the aforementioned non-rigid registration. The recurrent tumor was manually segmented in the same manner as the tumor segmentation on the pre-procedural image. The

3D distance between the local recurrence and the area with insufficient ablation margin (positive margin or thinnest margin) was measured by the following steps: 1) the 3D distance map from the area of insufficient margins were calculated; 2) the 3D distance map was overlaid on the segmentation of recurrent tumors; and 3) the minimum distance between the area of insufficient ablation and the local recurrence was calculated by finding the minimum value within the recurrent tumor on the distance map.

2.7 Statistical Analysis

DSC, percentage of target volume coverage, percentage of tumor coverage, tumor volume, and tumor diameter were compared between outcome groups using a two-sample t test. Complete tumor coverage of ablation zone was compared between the two outcome groups via Fishers exact test. Only two-sided p-values at preset with a significant (alpha) level of 0.05 were reported. All statistical analysis was performed in STATA Version 11.2 (StataCorp, College Station, TX).

3 Results

Representative results of image registration and visual assessment of pre- and post-procedural images and follow-up images are shown in Fig. 3. The target registration errors (TRE) were 2.23 ± 0.95 mm for pre- and post-procedural images, and 2.40 ± 0.35 mm for post-procedural and follow-up images based on landmarks manually defined in the liver regions. The result of ablation margin assessment with volumetric approach is shown in Table 2. Out of the 21 procedures, local recurrences were found in five cases. For the cases with recurrence, the pre-procedural tumor volume and the largest diameter were significantly higher than those for the cases without recurrence (21.7 ± 14.0 cm^3 vs 2.5 ± 2.2 cm^3 ($p < 0.001$) and 3.5 ± 0.6 cm vs 1.5 ± 0.9 cm ($p < 0.001$) respectively) (Table 3). The mean percent of tumor coverage for the cases with local recurrence was significantly lower than that of the other cases (99.7±0.3% vs 100.0 ± 0.3% ($p < 0.001$)). The DSC for the cases with local recurrence was higher than that for the cases without local recurrences (66.9 ± 8.0% vs 52.6± 8.4% ($p = 0.004$)). Of the 21 procedures, none of them had 100% target volume coverage (with 10 mm margin) by their ablation zones. Four procedures resulted in less than 100% coverage, and local recurrences were found in the all four cases. However, there was one recurrence with 100% tumor coverage. A branch of the portal vein with a diameter of 4.0 mm was adjacent to the tumor in this case.

The evaluation using the distance map showed that the thinnest margins for the five cases with recurrence were all zero, while the other cases without recurrence had thinnest margins of more than 1 mm. Distribution of ablation margin on the ablation volume surface and the relationship between the area of insufficient margin and the local recurrence are shown in Fig. 4. Three of five recurrences were found at the area of insufficient margin. One of the other two recurrent tumors was 2.7 cm away from the insufficient margin. The other recurrent case did not show the obvious positive margin, and the recurrent tumor was 2.7 cm away from the area of the insufficient margin.

4 Discussion

In this study, we demonstrated the feasibility of our method for quantitative assessment of ablation margin using non-rigid registration technique and 3D distance map, and its potential to predict local recurrence. When insufficient tumor coverage was found with non-rigid registration, a local recurrence was highly likely. Although we applied a 10-mm margin for the target volume as suggested by previous studies [51,38,1,16], it is rare to be able to achieve it in all directions due to anatomical restriction, such as contiguous organs and large vessels [31]. The 3D distance map enabled even more detailed analysis of the ablation margin; the result showed that the all cases with the thinnest margin of zero led to recurrences. Margins less than 10 mm might be reasonable for percutaneous liver ablation [31,18,44,23]. Compared to the distance-based assessment, % tumor coverage did not predict local recurrences well. % tumor coverage does not change from its maximum value (100) unless there is a positive margin; hence % tumor coverage of 100 cannot distinguish the thickness of margins. This is particularly problematic when the tumor and ablation volumes are very close, because variability of segmentation of tumor and ablation volume can turn < 100 % tumor coverage to 100.

Among the cases with local recurrences, the distance map revealed that three of the five were at the areas of insufficient margins. In two cases, recurrences were not at the areas of insufficient margins (Cases 2 and 5). These discordant results are likely due to the fact that recurrences can occur secondary to other factors such as adjacent large blood vessels [31,25] rather than insufficient ablation margins. In fact, a large branch of the portal vein was adjacent to the tumor in Case 2, in which a recurrence occurred without obvious insufficient margins. Studies have revealed that large vessels contiguous to hepatic tumors are likely to be a risk factor of local recurrence after liver ablation [31,25,26], and this might have led to recurrence in this case. In addition, non-rigid registration may not correct for the deformation of the liver completely; the treatment and/or changes in disease condition can change the liver shape significantly, making it difficult to register the pre- and post-procedural images and follow-up images. Local deformation of the liver due to shrinkage [41] and inflammatory response in the ablation area [5] and/or liver regeneration [42] may account for local recurrence distant from the insufficient ablation margin.

Blood vessels can cause insufficient ablation margins. Kim *et al* reported that blood vessels affected 50.5% (48/95 cases) of insufficient ablation margins [18]. In the representative case shown in Fig. 3, there was a right branch of portal vein on the inferior side, and a middle hepatic vein on the right side of the tumor. Since injuries of vessels had to be avoided, the tumor might have been insufficiently ablated near the hepatic vein.

Accurate registration is crucial for the distance-based ablation margin analysis. While our qualitative evaluation of registration by the clinicians were satisfactory, the TRE between the preprocedural, postprocedural, and follow-up images suggests that the registration error might not be ignorable. The slice thicknesses was not consistent in this study (2.0–4.0 mm) and larger thicknesses might have affected the registration error; using a smaller and consistent slice thickness could improve registration accuracy and hence reliability of result for the future prospective study.

Because this preliminary study was focused on correlation between the metrics for ablation margins and local recurrence, we applied rigorous exclusion criteria to eliminate all possible factors that could potentially confound our correlation. We excluded cases with unclear boundary of ablated areas, because they could cause inaccurate margin assessment. Similarly, we excluded tumors adjacent to the liver capsules, because they made it difficult to evaluate margins beyond liver surface. We excluded lesions within 1cm from other lesions treated previously, because they led to overlapped ablation volumes that would make the borders of ablation volume invisible. Target volumes overlapped with prior treatment area were also excluded, because they could also lead to invisible borders of ablation volumes.

The proposed analysis could be performed in conjunction with the existing clinical work flow. We considered the following clinical work flow: a) pre-procedural contrast-enhanced MRI within 30 days prior to ablation (day −30); b) ablation procedure (day 0); c) post-procedural contrast-enhanced MRI within 72hours following the treatment (day +1); d) ablation margin assessment when the physician is available (day +5); e) additional procedure is scheduled when insufficient ablation is identified; f) follow-up contrast-enhanced MRI done periodically after sufficient ablation (day 30 to 365). The assessment (step d) is the only step added to the regular clinical work flow; it can be performed offline, and typically requires only 10–15 minutes of manual tasks and 15 minutes of computation. Therefore, it would be feasible to perform the assessment in a clinical routine. The manual tasks include drawing of region of interest for liver registration (three to five minutes per liver), contouring of tumors and ablation volume (three to five minutes).

In our study, the average volume and the largest diameter of target tumors in recurrent cases were significantly larger than those of non-recurrent cases. Smaller tumor volume is considered important for curative treatment; complete ablation of a large tumor is often technically challenging and results in insufficient tumor coverage[48,31,15,21]. In fact, our quantitative margin assessment showed that ablation of large tumors resulted in insufficient margins (thinnest margin = 0 mm) in all 4/4. This result suggests that higher recurrence rates for large tumors might be associated with technical challenges to achieve complete ablation in this group. While the study did not assess sufficient number of samples, we believe that the proposed quantitative assessment method will help physicians determine if additional ablation procedure is necessary, and potentially reduce local recurrence after ablation of large tumors.

There are several limitations in our study. First, our sample size is limited due to our extensive exclusion criteria to be able to evaluate ablation margin accurately. Even though we reviewed 208 cases with different ablation modalities performed during the period of 5 years, we could only identify 21 cases that were suitable for our study. In particular, the availability of pre-procedural contrast-enhanced MR significantly reduced the sample size. Therefore, a future prospective study is crucial to ensure that all subjects undergo necessary examination before and after the treatment, and collect data effectively. Second, the ablation techniques were not uniform; three different ablation techniques, and three different image guidance modalities were included in the study. Tissue viability at the edge of ablation volume detected on the post-procedural image may differ between the ablation techniques [7]. Origin or pathological character of tumors might also affect the local recurrence rate

because recurrence patterns are different between tumor types [14, 3,34], but we could not compare the recurrence rates between different origins or pathological characters due to the limited sample size. Further evaluation of the method with a larger cohort would help understand the effectiveness of our method in predicting the local recurrence. Such a cohort would also allow us to compare the proposed method to the qualitative evaluation by radiologists. Third, variability in the manual segmentation of tumor and ablation volume might have degraded the accuracy of margin assessment. In the future, automatic segmentation would improve the assessment time and repeatability. In particular, automatic segmention of tumor and ablation volume by comparing the baseline and hepatobiliary-phase on Gd-EOB-DTPA-based contrast-enhanced MR images would be of our interest. The technique could also be useful for monitoring the progress of ablation in real-time during the procedure. For example, the technique could be combined with intraprocedural non-rigid image registration for intraprocedure margin assessment [10, 37,49], MR thermometry for microwave ablation monitoring[30], MR-based ice ball monitoring for MRI-guided cryoablations[24]. In addition, the method could potentially integrated with other real-time imaging modalities such as contrast-enhanced ultrasound [52,6].

In conclusion, non-rigid registration and the 3D distance map allows us to quantitatively evaluate the adequacy of ablation margin after percutaneous liver ablation. This technique may be used to predict local recurrences at an early point in time even immediately following an ablation procedure and improve patient care.

Acknowledgments

The authors would like to thank Vincent M. Levesque for his assistance in collecting patient data.

Funding This study was supported by the National Institutes of Health (R01CA138586, P41EB015898, P41EB015898). S. Tani received funds from the Ministry of Education, Culture, Sports, Science, and Technology, Japan. The content of the material is solely the responsibility of the authors and does not necessarily represent the official views of these agencies.

References

1. Bowles BJ, Machi J, Limm WM, Severino R, Oishi aJ, Furumoto NL, Wong LL, Oishi RH. Safety and efficacy of radiofrequency thermal ablation in advanced liver tumors. Archives of surgery (Chicago, Ill: 1960). 2001; 136(8):864–9.
2. Carrillo A, Duerk JL, Lewin JS, Wilson DL. Semiautomatic 3-D image registration as applied to interventional MRI liver cancer treatment. IEEE Transactions on Medical Imaging. 2000; 19(3): 175–185. DOI: 10.1109/42.845176 [PubMed: 10875702]
3. Chambers AF, Groom AC, MacDonald IC. Dissemination and growth of cancer cells in metastatic sites. Nature reviews. Cancer. 2002; 2(8):563–72. DOI: 10.1038/nrc865 [PubMed: 12154349]
4. Chopra S, Dodd GD, Chintapalli KN, Leyendecker JR, Karahan OI, Rhim H. Tumor Recurrence After Radiofrequency Thermal Ablation of Hepatic Tumors Spectrum of Findings on Dual-Phase Contrast-Enhanced CT. American Journal of Roentgenology. 2001; 177(2):381–387. [PubMed: 11461868]
5. Chu KF, Dupuy DE. Thermal ablation of tumours: biological mechanisms and advances in therapy. Nature Reviews Cancer. 2014; 14(3):199–208. DOI: 10.1038/nrc3672 [PubMed: 24561446]
6. Claudon M, Dietrich CF, Choi BI, Cosgrove DO, Kudo M, Nolsøe CP, Piscaglia F, Wilson SR, Barr RG, Chammas MC, Chaubal NG, Chen MH, Clevert DA, Correas JM, Ding H, Forsberg F, Fowlkes JB, Gibson RN, Goldberg BB, Lassau N, Leen ELS, Mattrey RF, Moriyasu F, Solbiati L, Weskott HP, Xu HX. Guidelines and Good Clinical Practice Recommendations for Contrast Enhanced

Ultrasound (CEUS) in the Liver - Update 2012. A WFUMB-EFSUMB Initiative in Cooperation with Representatives of AFSUMB, AIUM, ASUM, FLAUS and ICUS. Ultrasound in Medicine and Biology. 2013; 39(2):187–210. DOI: 10.1016/j.ultrasmedbio.2012.09.002 [PubMed: 23137926]

7. Delis S, Bramis I, Triantopoulou C, Madariaga J, Dervenis C. The imprint of radiofrequency in the management of hepatocellular carcinoma. HPB: Official Journal of The International Hepato Pancreato Biliary Association. 2006; 8(4):255–263. DOI: 10.1080/13651820500273673
8. Dodd GD, Soulen MC, Kane RA, Livraghi T, Lees WR, Yamashita Y, Gillams aR, Karahan OI, Rhim H. Minimally invasive treatment of malignant hepatic tumors: at the threshold of a major breakthrough. Radiographics : a review publication of the Radiological Society of North America, Inc. 2000; 20(1):9–27. DOI: 10.1148/radiographics.20.1.g00ja019
9. El-Serag HB. Hepatocellular carcinoma. The New England journal of medicine. 2011; (12):1118–27. DOI: 10.1056/NEJMra1001683 [PubMed: 21992124]
10. Elhawary H, Oguro S, Tuncali K, Morrison PR, Tatli S, Shyn PB, Silverman SG, Hata N. Multimodality non-rigid image registration for planning, targeting and monitoring during CT-guided percutaneous liver tumor cryoablation. Academic radiology. 2010; 17(11):1334–44. DOI: 10.1016/j.acra.2010.06.004 [PubMed: 20817574]
11. Fedorov A, Tuncali K, Fennessy FM, Tokuda J, Hata N, Wells WM, Kikinis R, Tempany CM. Image registration for targeted MRI-guided transperineal prostate biopsy. Journal of Magnetic Resonance Imaging. 2012; 36(4):987–992. DOI: 10.1002/jmri.23688 [PubMed: 22645031]
12. Fujioka C, Horiguchi J, Ishifuro M, Kakizawa H, Kiguchi M, Matsuura N, Hieda M, Tachikake T, Alam F, Furukawa T, Ito K. A Feasibility Study: Evaluation of Radiofrequency Ablation Therapy to Hepatocellular Carcinoma Using Image Registration of Preoperative and Postoperative CT. Academic Radiology. 2006; 13(8):986–994. DOI: 10.1016/j.acra.2006.05.011 [PubMed: 16843851]
13. Goldberg SN, Charboneau JW, Dodd GD, Dupuy DE, Gervais DA, Gillams AR, Kane RA, Lee FT, Livraghi T, McGahan JP, Rhim H, Silverman SG, Solbiati L, Vogl TJ, Wood BJ. Image-guided Tumor Ablation: Proposal for Standardization of Terms and Reporting Criteria1. Radiology. 2003; 228(2):335–345. DOI: 10.1148/radiol.2282021787 [PubMed: 12893895]
14. Hess KR, Varadhachary GR, Taylor SH, Wei W, Raber MN, Lenzi R, Abbruzzese JL. Metastatic patterns in adenocarcinoma. Cancer. 2006; 106(7):1624–1633. DOI: 10.1002/cncr.21778 [PubMed: 16518827]
15. Hori T, Nagata K, Hasuike S, Onaga M, Motoda M, Moriuchi A, Iwakiri H, Uto H, Kato J, Ido A, Hayashi K, Tsubouchi H. Risk factors for the local recurrence of hepatocellular carcinoma after a single session of percutaneous radiofrequency ablation. Journal of Gastroenterology. 2003; 38(10): 977–981. DOI: 10.1007/s00535-003-1181-0 [PubMed: 14614605]
16. Kettenbach J, Köstler W, Rücklinger E, Gustorff B, Hüpfl M, Wolf F, Peer K, Weigner M, Lammer J, Müller W, Goldberg SN. Percutaneous saline-enhanced radiofrequency ablation of unresectable hepatic tumors: Initial experience in 26 patients. American Journal of Roentgenology. 2003; 180(June):1537–1545. DOI: 10.2214/ajr.180.6.1801537 [PubMed: 12760914]
17. Kim KW, Lee JM, Klotz E, Kim SJ, Kim SH, Kim JY, Han JK, Choi BI. Safety margin assessment after radiofrequency ablation of the liver using registration of preprocedure and postprocedure CT images. American Journal of Roentgenology. 2011; 196(5):565–572. DOI: 10.2214/AJR.10.5122
18. Kim YS, Lee WJ, Rhim H, Lim HK, Choi D, Lee JY. The minimal ablative margin of radiofrequency ablation of hepatocellular carcinoma (> 2 and < 5 cm) needed to prevent local tumor progression: 3D quantitative assessment using CT image fusion. AJR. American journal of roentgenology. 2010; 195(September):758–765. DOI: 10.2214/AJR.09.2954 [PubMed: 20729457]
19. Kim, Ys; Rhim, H.; Cho, OK.; Koh, BH.; Kim, Y. Intrahepatic recurrence after percutaneous radiofrequency ablation of hepatocellular carcinoma: analysis of the pattern and risk factors. European journal of radiology. 2006; 59(3):432–41. DOI: 10.1016/j.ejrad.2006.03.007 [PubMed: 16690240]
20. Koda M, Tokunaga S, Miyoshi K, Kishina M, Fujise Y, Kato J, Matono T, Okamoto K, Murawaki Y, Kakite S. Assessment of ablative margin by un-enhanced magnetic resonance imaging after radiofrequency ablation for hepatocellular carcinoma. European Journal of Radiology. 2012; 81(10):2730–2736. DOI: 10.1016/j.ejrad.2011.11.013 [PubMed: 22137612]

21. Komorizono Y, Oketani M, Sako K, Yamasaki N, Shibatou T, Maeda M, Kohara K, Shigenobu S, Ishibashi K, Arima T. Risk factors for local recurrence of small hepatocellular carcinoma tumors after a single session, single application of percutaneous radiofrequency ablation. Cancer. 2003; 97(5):1253–62. DOI: 10.1002/cncr.11168 [PubMed: 12599233]
22. Leung U, Kuk D, D'angelica MI, Kingham TP, Allen PJ, Dematteo RP, Jarnagin WR, Fong Y. Long-term outcomes following microwave ablation for liver malignancies. The British Journal of Surgery. 2014; 102(1):85–91. DOI: 10.1002/bjs.9649 [PubMed: 25296639]
23. Liu CH, Arellano RS, Uppot RN, Samir AE, Gervais Da, Mueller PR. Radiofrequency ablation of hepatic tumours: effect of post-ablation margin on local tumour progression. European radiology. 2010; 20(4):877–85. DOI: 10.1007/s00330-009-1610-4 [PubMed: 19760232]
24. Liu X, Tuncali K, Wells WM, Zientara GP. Automatic iceball segmentation with adapted shape priors for MRI-guided cryoablation. Journal of Magnetic Resonance Imaging. 2015; 41(2):517–524. DOI: 10.1002/jmri.24531 [PubMed: 24338961]
25. Lu DS, Raman SS, Limanond P, Aziz D, Economou J, Busuttil R, Sayre J. Influence of Large Peritumoral Vessels on Outcome of Radiofrequency Ablation of Liver Tumors. Journal of Vascular and Interventional Radiology. 2003; 14(10):1267–1274. DOI: 10.1097/01.RVI.0000092666.72261.6B [PubMed: 14551273]
26. Machi J, Uchida S, Sumida K, Limm WM, Hundahl SA, Oishi AJ, Furumoto NL, Oishi RH. Ultrasound-guided radiofrequency thermal ablation of liver tumors: percutaneous, laparoscopic, and open surgical approaches. Journal of gastrointestinal surgery : official journal of the Society for Surgery of the Alimentary Tract. 2001; 5(5):477–89. [PubMed: 11985998]
27. Martin RCG, Scoggins CR, McMasters KM. Safety and Efficacy of Microwave Ablation of Hepatic Tumors: A Prospective Review of a 5-Year Experience. Annals of Surgical Oncology. 2010; 17(1):171–178. DOI: 10.1245/s10434-009-0686-z [PubMed: 19707829]
28. Maurer C, Raghavan V. A linear time algorithm for computing exact Euclidean distance transforms of binary images in arbitrary dimensions. IEEE Transactions on Pattern Analysis and Machine Intelligence. 2003; 25(2):265–270. DOI: 10.1109/TPAMI.2003.1177156
29. Mori K, Fukuda K, Asaoka H, Ueda T, Kunimatsu A, Okamoto Y, Nasu K, Fukunaga K, Morishita Y, Minami M. Radiofrequency ablation of the liver: determination of ablative margin at MR imaging with impaired clearance of ferucarbotran–feasibility study. Radiology. 2009; 251(2):557–565. DOI: 10.1148/radiol.2512081161 [PubMed: 19251941]
30. Morikawa S, Inubushi T, Kurumi Y, Naka S, Sato K, Demura K, Tani T, Haque HA, Tokuda J, Hata N. Advanced Computer Assistance for Magnetic Resonance-Guided Microwave Thermocoagulation of Liver Tumors. Academic Radiology. 2003; 10(12):1442–1449. DOI: 10.1016/S1076-6332(03)00508-7 [PubMed: 14697012]
31. Mulier S, Ni Y, Jamart J, Ruers T, Marchal G, Michel L. Local Recurrence After Hepatic Radiofrequency Coagulation. Annals of Surgery. 2005; 242(2):158–171. DOI: 10.1097/01.sla.0000171032.99149.fe [PubMed: 16041205]
32. Nakazawa T, Kokubu S, Shibuya A, Ono K, Watanabe M, Hidaka H, Tsuchihashi T, Saigenji K. Radiofrequency ablation of hepatocellular carcinoma: correlation between local tumor progression after ablation and ablative margin. AJR. American journal of roentgenology. 2007; 188(2):480–488. DOI: 10.2214/AJR.05.2079 [PubMed: 17242258]
33. Ng KK, Poon RT, Lo CM, Yuen J, Tso WK, Fan ST. Analysis of recurrence pattern and its influence on survival outcome after radiofrequency ablation of hepatocellular carcinoma. Journal of Gastrointestinal Surgery. 2008; 12(1):183–191. DOI: 10.1007/s11605-007-0276-y [PubMed: 17874276]
34. Nguyen DX, Bos PD, Massagué J. Metastasis: from dissemination to organ-specific colonization. Nature reviews. Cancer. 2009; 9(4):274–284. DOI: 10.1038/nrc2622 [PubMed: 19308067]
35. Niculescu, G.; Foran, DJ.; Nosher, J. Non-rigid registration of the liver in consecutive CT studies for assessment of tumor response to radiofrequency ablation. Engineering in Medicine and Biology Society, 2007. EMBS 2007. 29th Annual International Conference of the IEEE; 2007. p. 856-9.
36. Oguro S, Tokuda J, Elhawary H, Haker S, Kikinis R, Tempany CMC, Hata N. MRI signal intensity based B-spline nonrigid registration for pre- and intraoperative imaging during prostate

brachytherapy. Journal of magnetic resonance imaging : JMRI. 2009; 30(5):1052–8. DOI: 10.1002/jmri.21955 [PubMed: 19856437]

37. Oguro S, Tuncali K, Elhawary H, Morrison PR, Hata N, Silverman SG. Image registration of pre-procedural MRI and intra-procedural CT images to aid CT-guided percutaneous cryoablation of renal tumors. International Journal of Computer Assisted Radiology and Surgery. 2011; 6(1):111–117. DOI: 10.1007/s11548-010-0485-9 [PubMed: 20499194]
38. Pawlik TM, Izzo F, Cohen DS, Morris JS, Curley SA. Combined resection and radiofrequency ablation for advanced hepatic malignancies: results in 172 patients. Annals of surgical oncology. 2003; 10(9):1059–1069. DOI: 10.1245/ASO.2003.03.026 [PubMed: 14597445]
39. Ravikumar TS. A 5-Year Study of Cryosurgery in the Treatment of Liver Tumors. Archives of Surgery. 1991; 126(12):1520.doi: 10.1001/archsurg.1991.01410360094015 [PubMed: 1842183]
40. Rossi S, Di Stasi M, Buscarini E, Quaretti P, Garbagnati F, Squassante L, Paties CT, Silverman DE, Buscarini L. Percutaneous RF interstitial thermal ablation in the treatment of hepatic cancer. American Journal of Roentgenology. 1996; 167(3):759–768. DOI: 10.2214/ajr.167.3.8751696 [PubMed: 8751696]
41. Rossmann C, Garrett-Mayer E, Rattay F, Haemmerich D. Dynamics of tissue shrinkage during ablative temperature exposures. Physiological measurement. 2014; 35(1):55–67. DOI: 10.1088/0967-3334/35/1/55 [PubMed: 24345880]
42. Rozenblum N, Zeira E, Bulvik B, Gourevitch S, Yotvat H, Galun E, Goldberg SN. Radiofrequency Ablation: Inflammatory Changes in the Periablative Zone Can Induce Global Organ Effects, including Liver Regeneration. Radiology. 2015; 276(2):416–25. DOI: 10.1148/radiol.15141918 [PubMed: 25822472]
43. Shibata T, Iimuro Y, Yamamoto Y, Maetani Y, Ametani F, Itoh K, Konishi J. Small hepatocellular carcinoma: comparison of radiofrequency ablation and percutaneous microwave coagulation therapy. Radiology. 2002; 223(2):331–7. DOI: 10.1148/radiol.2232010775 [PubMed: 11997534]
44. Shyn PB, Mauri G, Alencar RO, Tatli S, Shah SH, Morrison PR, Catalano PJ, Silverman SG. Percutaneous imaging-guided cryoablation of liver tumors: predicting local progression on 24-hour MRI. AJR. American journal of roentgenology. 2014; 203(2):W181–91. DOI: 10.2214/AJR.13.10747 [PubMed: 24555531]
45. Silverman SG, Sun MRM, Tuncali K, Morrison PR, VanSonnenberg E, Shankar S, Zou KH, Warfield SK. Three-dimensional assessment of MRI-guided percutaneous cryotherapy of liver metastases. AJR. American journal of roentgenology. 2004; 183(3):707–12. DOI: 10.2214/ajr.183.3.1830707 [PubMed: 15333359]
46. Silverman SG, Tuncali K, Adams DF, VanSonnenberg E, Zou KH, Kacher DF, Morrison PR, Jolesz FA. MR Imaging-guided Percutaneous Cryotherapy of Liver Tumors: Initial Experience1. Radiology. 2000; 217(3):657–664. DOI: 10.1148/radiology.217.3.r00dc40657 [PubMed: 11110925]
47. Stewart, BW.; Wild, CP. International Agency for Research on Cancer. WHO; 2014. World Cancer Report 2014. 9283204298
48. Tateishi R, Shiina S, Teratani T, Obi S, Sato S, Koike Y, Fujishima T, Yoshida H, Kawabe T, Omata M. Percutaneous radiofrequency ablation for hepatocellular carcinoma: An analysis of 1000 cases. Cancer. 2005; 103(6):1201–1209. DOI: 10.1002/cncr.20892 [PubMed: 15690326]
49. Tokuda J, Plishker W, Torabi M, Olubiyi OI, Zaki G, Tatli S, Silverman SG, Shekher R, Hata N. Graphics Processing UnitAccelerated Nonrigid Registration of MR Images to CT Images During CT-Guided Percutaneous Liver Tumor Ablations. Academic Radiology. 2015; 22(6):722–733. DOI: 10.1016/j.acra.2015.01.007 [PubMed: 25784325]
50. Wilson DL, Carrillo A, Zheng L, Genc A, Duerk JL, Lewin JS. Evaluation of 3D image registration as applied to MR-guided thermal treatment of liver cancer. Journal of Magnetic Resonance Imaging. 1998; 8(1):77–84. [PubMed: 9500264]
51. Wood TF, Rose DM, Chung M, Allegra DP, Foshag LJ, Bilchik aJ. Radiofrequency ablation of 231 unresectable hepatic tumors: indications, limitations, and complications. Annals of surgical oncology. 2000; 7(8):593–600. [PubMed: 11005558]

52. Wu H, Wilkins LR, Ziats NP, Haaga JR, Exner AA. Real-time monitoring of radiofrequency ablation and postablation assessment: accuracy of contrast-enhanced US in experimental rat liver model. Radiology. 2014; 270(1):107–16. DOI: 10.1148/radiol.13121999 [PubMed: 23912621]

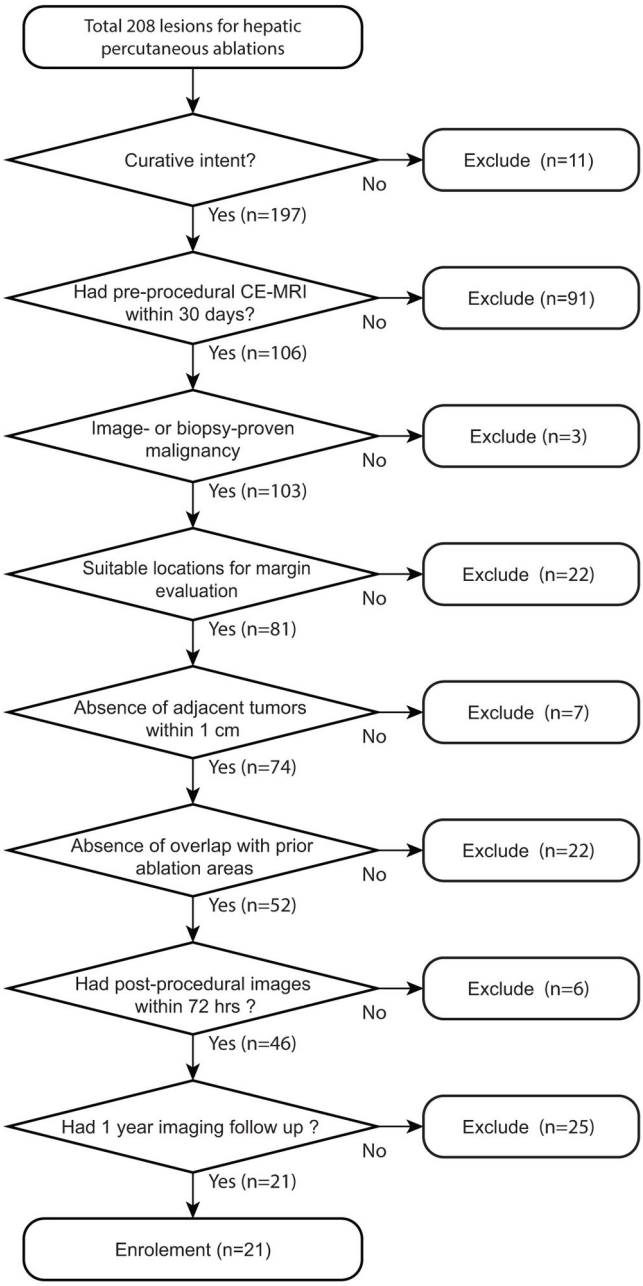

Fig. 1.

Flowchart of inclusion criteria. The top box demonstrates the number of patients who underwent percutaneous liver ablation between January 1, 2008 and December 31, 2012.

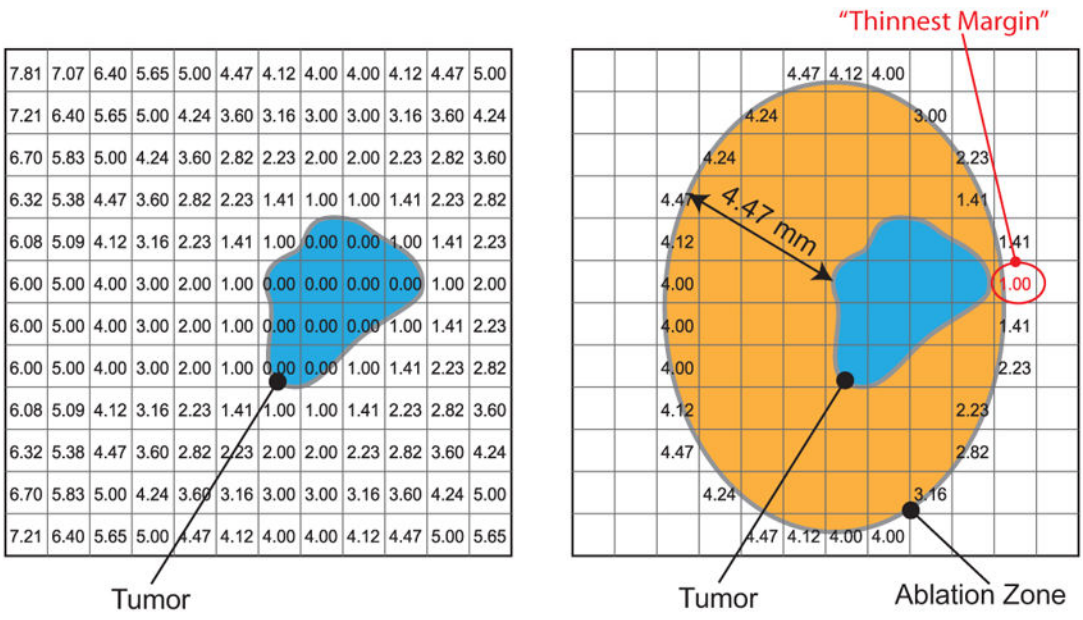

Fig. 2.

Schematic 2D representation of ablation margin assessment using a distance map is shown. A distance map, which contains the minimum distances from the tumor region to each pixel, is calculated (left), and then superimposed on the ablation zone (right). The values in the pixels at the boundary of ablation zone represent the minimum distances from the tumor surface, hence these pixel values represent the thickness of ablation margin. The pixel with the minimum value represents the point of thinnest margin. In our analysis, a 3D distance map with a pixel size of 1 × 1 × 1 mm was used.

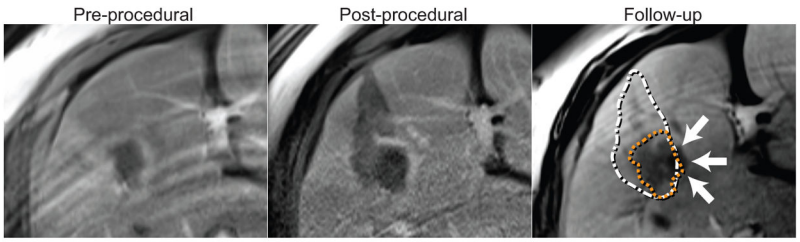

Fig. 3.

Co-registered pre-procedural, post-procedural, and follow-up CE-MR images show tumor, ablation volume, and recurrence respectively (Case 14). The orange and white dotted line superimposed on the follow-up image represents the locations of the tumor and the ablation zone. The recurrence indicated by the arrows is observed at the area with positive ablation margin.

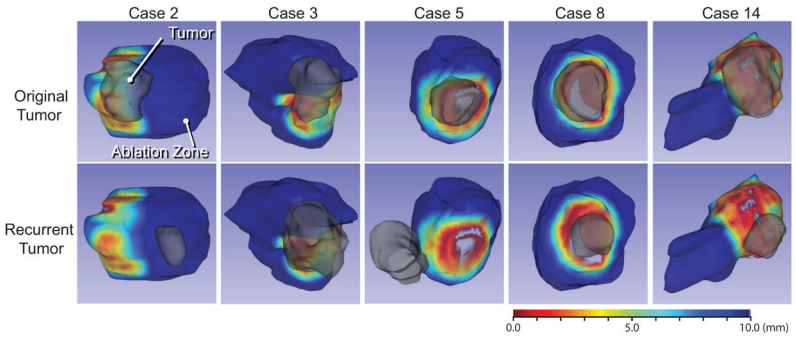

Fig. 4.

Three-dimensional color maps of distance map between the original tumor and ablation zone are rendered on the surface of ablation zone for the cases with local recurrences. The red areas represent insufficient ablation margin. The 3D models of original (upper) and recurrent (lower) tumors are superimposed. The red areas represent ablation margins with a thickness close to zero.

Table 1

Characteristics of 21 cases that met the inclusion criteria including the origin of malignancy for primary and metastatic tumors (Malignancy Origin) and the diameters of tumors. The primary origin of the hepatic malignancies included gastrointestinal stromal tumors (n=2), hepatocellular carcinoma (n=3), colorectal carcinoma (n=9), esophageal carcinoma (n=2), uterine sarcoma (n=1), carcinoid (n=1), thymoma (n=1), renal cell carcinoma (n=1), and endometrial carcinoma (n=1).

Case	Ablation Modality	Malignancy Origin	Tumor Diameter (cm)
1	Cryo	Colon	1.0
2	Cryo	Esophagus	3.2
3	RFA	GIST	2.1
4	Cryo	HCC	1.3
5	Cryo	HCC	4.0
6	RFA	Esophagus	1.8
7	Cryo	Uterine sarcoma	1.0
8	Cryo	Colon	4.0
9	RFA	Colon	2.8
10	RFA	GIST	1.5
11	RFA	HCC	1.4
12	RFA	Carcinoid	1.7
13	Cryo	Thymoma	1.1
14	MCT	Colon	4.1
15	Cryo	Colon	0.9
16	Cryo	Colon	2.0
17	Cryo	RCC	1.1
18	Cryo	Colon	1.6
19	MCT	Colon	2.7
20	RFA	Endometrial Carcinoma	1.0
21	Cryo	Colon	0.9

Cryo: cryoablation; RFA: radiofrequency ablation; MCT: microwave coagulation therapy; GIST: gastrointestinal stromal tumor; HCC: hepatocellular carcinoma.

Table 2

Metrics for ablation volume assessment including tumor volume, percent tumor volume coverage, percent target volume coverage, DSC, thinnest margin, and follow-up results. For cases with recurrences, the minimum distance between the insufficient margin to the recurrence is also shown. Note that the thinnest margin between 0.0 mm and 1.1 are shown as "≤1.0", because the margins were calculated based on a 3D distance map with 1-mm isotropic voxels; the minimum non-zero distance in such a distance map was 1.0.

Case	Tumor Volume (cm^3)	%Tumor Coverage	%Target Coverage	DSC	Thinnest Margin (mm)	Recurrence	Distance insuff. margin (cm)
1	0.4	100	99.9	0.63	7.8	No	
2	13.3	100	84.1	0.66	0.0	Yes	2.7
3	7.9	99.9	76.8	0.58	0.0	Yes	0.0
4	1.1	100	95.2	0.63	5.1	No	
5	14.1	99.2	85.2	0.67	0.0	Yes	2.7
6	3.2	100	87.4	0.53	1.7	No	
7	1.0	100	94.0	0.51	5.0	No	
8	40.2	99.5	89.8	0.79	0.0	Yes	0.0
9	7.9	100	92.9	0.66	1.4	No	
10	2.2	100	77.5	0.47	1.4	No	
11	2.4	100	99.2	0.46	6.2	No	
12	2.5	100	98.3	0.61	3.2	No	
13	1.7	100	93.7	0.36	4.1	No	
14	32.9	99.6	72.9	0.63	0.0	Yes	0.0
15	1.1	100	99.2	0.42	6.1	No	
16	4.9	100	99.8	0.42	6.7	No	
17	1.0	100	66.9	0.51	≤ 1.0	No	
18	2.5	100	66.6	0.56	≤ 1.0	No	
19	6.6	100	89.6	0.55	≤ 1.0	No	
20	1.2	100	80.6	0.47	≤ 1.0	No	
21	0.8	100	95.7	0.59	4.1	No	

Distance insuff. margin: minimum distance between the recurrence and the area with insufficient margin;

Table 3

Summary of tumor size, and ablation coverlage

	Positive	Negative	p-value
Tumor diameter (cm)	3.5 ± 0.6	1.5 ± 0.9	< 0.001
Tumor volume (cm^3)	21.7 ± 14.0	2.5 ± 2.2	< 0.001
Tumor coverage	99.6 ± 0.3	100.0 ± 0	< 0.001
Target coverage	81.9 ± 6.8	89.7 ± 11.1	0.15
Total tumor coverage	1 (of 5)	16 (of 16)	0.001
DSC	0.67 ± 0.08	0.52 ± 0.09	0.004